Polarforschung 62 (2/3): 71–76, 1992 (erschienen 1994)

Bottom Melting on the Filchner-Ronne Ice Shelf, Antarctica, Using Different Measuring Techniques

By Klaus Grosfeld, Norbert Blindow and Franz Thyssen*

Summary: During the 1989/90 field season on Filchner-Ronne Ice Shelf (FRIS), Antarctica, special interest was focussed on the examination of the bottom-melting rate by different measuring techniques. Access to the sea water underneath the ice shelf was gained by means of hot-water drillings. The installation of temperature cable and TDR-sensor lines yield a distinct value of the bottom mass-balance parameter after re-measurement in 1992. In addition a seasonal dependence for bottom melting is indicated. The results of the long-term observation conform with a mass-balance study performed in the same region from surface-based measurements in the same season (DETERMANN et al. 1990). The influence of tidal-induced ice shelf/ocean interaction with regard to bottom melting can be derived from a continual registration of sea-water temperatures.

Zusammenfassung: In der vorgestellten Arbeit werden Ergebnisse von Untersuchungen auf dem Filchner-Ronne Schelfeis (FRIS), Antarktis, aufgezeigt, mit denen die basale Schmelzrate durch verschiedene, voneinander unabhängige Verfahren bestimmt worden ist. Im Jahr 1990 wurden hierzu Temperaturmeßketten und TDR-Sensorleitungen in Schmelzbohrlöcher eingebracht, die während einer zweiten Meßkampagne 1992 nachgemessen werden konnten. Die Messungen ergeben einen übereinstimmenden Mittelwert der basalen Schmelzrate im Kantenbereich des FRIS und liefern darüber hinaus Hinweise auf eine saisonale Abhängigkeit dieser wichtigen Massenbilanzgröße. Ein Vergleich mit einer von der Eisoberfläche durchgeführten Massenbilanzstudie im selben Meßgebiet (DETERMANN et al. 1990) liefert übereinstimmende Ergebnisse. Desweiteren konnten durch eine Dauerregistrierung der Meerwassertemperatur unterhalb des Schelfeises Hinweise auf Gezeiteneffekte in der Wechselwirkung zwischen Ozean und Schelfeis festgestellt werden.

INTRODUCTION

The bottom melting rate of ice shelves is a significant parameter for mass-balance studies but at the same time the most unknown parameter. Since 44 % of the Antarctic coast line is fringed by ice shelves (DREWRY et al. 1982), which represent the drainage basins of the Antarctic ice cap, the bottom melting rate is, in addition to the calving of icebergs, the only parameter on the net deficit site. Until now it has been calculated from surface measurements by indirect methods using continuity and isostatics. For different locations close to the ice-shelf edge of the Filchner-Ronne Ice Shelf (FRIS), melting rates were derived from BEHRENDT (1970) to -9m/a and KOHNEN (1982) to -3m/a, while JENKINS & DOAKE (1991) found magnitudes of -4m/a near the grounding line of Rutford Ice Stream. These values show the large variability and the importance of a reliable determination of this quantity. Although there are different causes producing basal melting at the grounding line and at the ice front, the knowlege of the quantity itself is necessary for mass balance studies and can hold for the validation of model results, describing ice-ocean interactions.

During the German Antarctic Expedition (ANT-VIII/5) 1989/90 hot-water drilling was performed 30 km inland from the ice front and 50 km north-west of the Filchner Station at 77° S and 52.3° W to investigate the ice thickness and its variation by temperature and time-domain reflectometry (TDR) measurements (GROSFELD 1993, GROSFELD & BLINDOW 1993). Re-measurements of the installed chains in 1991/92 yield a direct comparison for the change of the ice-shelf bottom over two years. In addition surface measurements of the components of the mass-balance equation gave a certain value for the bottom-melting rate (DETERMANN et al. 1990).

TEMPERATURE MEASUREMENTS

In 1990 five chains with 64,100 Ω Platinum RTD temperature sensors (PT100, type W60/30, Degussa) were frozen into the 239 ±2 m thick ice shelf to investigate the temperature-depth profile with regard to bottom melting and to thermal modelling of the central part of FRIS. The spacing of the PT100-sensors varies between 2 m near the ice surface, the meteoric/marine transition and the ice shelf bottom, 5 m within the marine layer and 10 m in the remaining ice shelf. The temperature data were calculated from resistivity measurements with a digital instrument (Keithley 197). The absolute accuracy of the sensors is ±0.1 K while relative resolution from resistivity measurements is better than 0.003 K .

The results of a two-years re-measurement 1990 (broken line) and 1992 (solid line) and their difference are shown in Figure 1. The upper 8 m of the temperature profiles (left) are influenced from the warm summer period and show a steep negative gradient. The heat input from 20 m to 50 m depth caused by the lateral penetration of the watertable from hot-water drilling in 1990 (broken line) has completely disappeared. Further down the temperature profiles show a uniform gradient. There are no differences between the temperature gradients in the meteoric and the marine ice, indicating similar heat conductivities and so equal thermal properties for both media. The marine ice layer originates from cristallisation processes in the ocean and reaches

* Dr. Klaus Grosfeld**, Dr. Norbert Blindow and Prof. Dr. Franz Thyssen, Forschungsstelle für physikalische Glaziologie, Universität Münster, Correnssstraße 24, D-48149 Münster.
** Present address: Alfred Wegener Institute for Polar and Marine Research, P.O. Box 12 01 61, D-27515 Bremerhaven.
Manuscript received 8 June 1993; accepted 16 December 1993

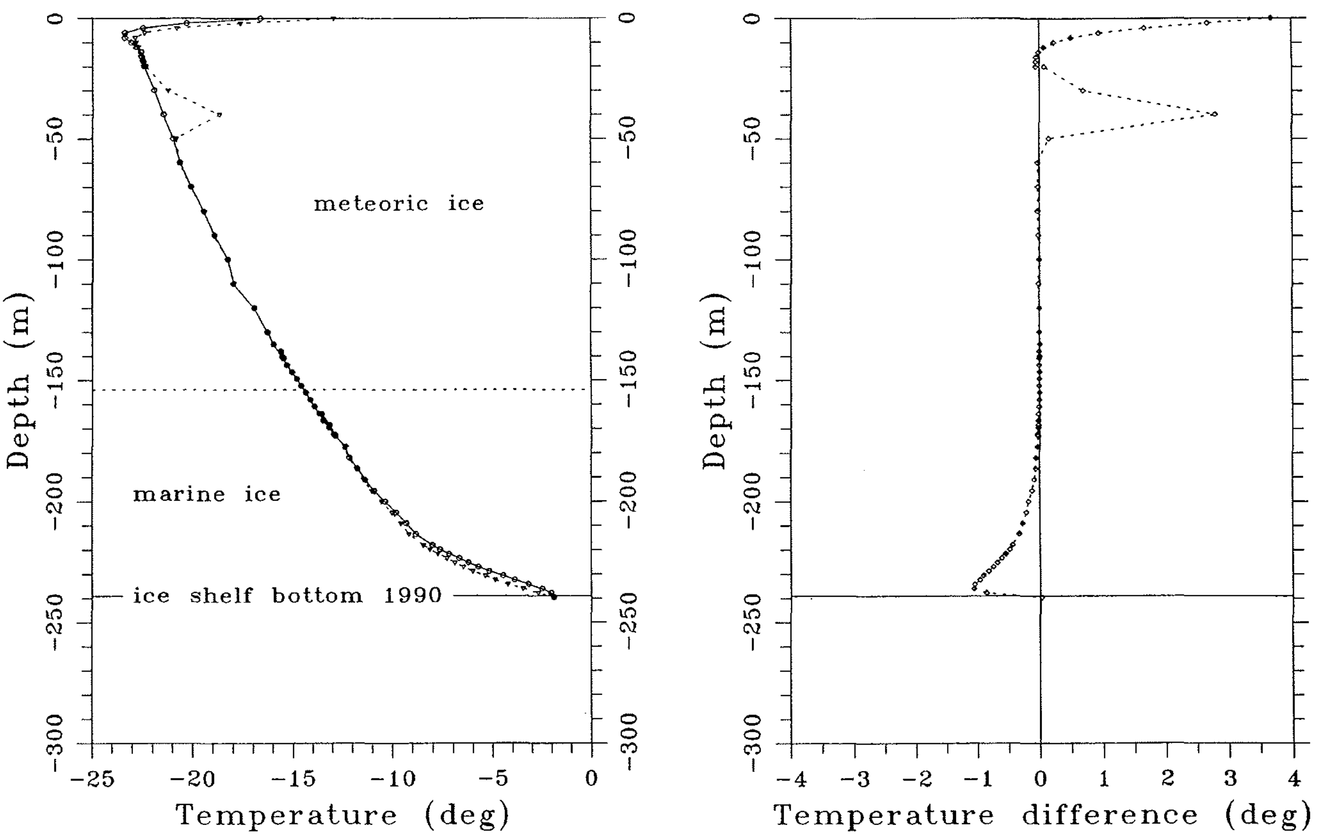

Fig. 1: Temperature-depth profile (left) on 13-02-1990 (broken line) and on 20-02-1992 (solid line) at the ice edge of FRIS, 50 km north-west of Filchner station, and their difference (right).

Abb. 1: Temperatur-Tiefenprofile (links) vom 13.02.1990 (gestrichelte Linie) und vom 20.02.1992 (durchgezogene Linie) im Eiskantenbereich des FRIS, 50km nordwestlich der Filchner-Station, und Differenz der Meßkurven (rechts).

a thickness of up to 400 m in the central part of the FRIS (THYSSEN 1988). Hence, it is a significant factor influencing the mass balance and dynamic of the whole ice shelf. Only the lowest 25 m above the ice-shelf bottom are influenced by bottom-melting processes and show a steeper temperature gradient. The influence of the heat input from bottom accretion in the central part of the FRIS, which causes an inversion in the temperature gradient (GROSFELD 1993), is eroded at this location, 30 km from the ice edge. The temperature profile shows a typical convex form, indicating basal melting processes.

In the main part of the temperature-depth profile (from 60 m to 200 m) the temperature difference between the data sets measured in 1990 and 1992 is very small (-0.024 ±0.026 K, Fig. 1 right), which confirms the long-term stability and accuracy of the PT100-sensors. Indeed, the steady state temperature was not reached again at the end of the field season 1990, but these temperature values could be calculated from a diagram of temperature versus a reciprocal time scale. A comparison of the extrapolated values with the measured data of 1990 show a difference of -0.103 ±0.027 K, which is within the error limit of the absolute accurary of the PT100-sensors. In the lowest part of the borehole (>200m depth) the temperature difference is more than 1 K, indicating the effect of bottom melting.

From these data the amount of bottom melting over two years can be determined by two methods: In 1990 only one PT100-sensor was placed in the sea water underneath the ice shelf. Two years later, the next sensor with a spacing of 2 m was melted out. From this, it is possible to directly derive the bottom-melting rate m to be -1.0 m/a ≥ m > -2.0 m/a. A detailed examination of the temperature gradient of the lowest PT100-sensors can give a more exact melting rate. Using the freezing point of the sea water underneath the ice shelf, the depth of the ice-shelf bottom can be calculated from the temperature boundary condition. According to FOLDVIK & KVINGE (1974) the freezing point of sea water at the ice/sea-water interface is given by $T_f = -0.057 \bullet S_b + 0.0939 - 7.64 \bullet 10^{-4} \bullet P$, where S_b is the salinity of sea water in ‰ and P is the pressure at the interface in dbar. Using typical salinity data for the southern Weddell Sea along the Filchner-Ronne ice front between 34.5 ‰ and 34.7 ‰ in about 200 m depth (FOLDVIK et al. 1985), freezing-point temperatures of -2.030 ±0.006° C were determined for the ice-shelf bottom. From polynomial interpolation of the temperature data in the lower part of the ice shelf, the ice/sea-water boundary was calculated to be 239.20 ±0.01 m in 1990 and 236.62 ±0.01 m in 1992 for the evaluated temperature range due to different salinities. The resulting melting rate over a period of 737 days is calculated to be m = -1.28 ±0.24 m/a, the error estimation is given by the residual sums of squares of the polynomial fit.

The same procedure was applied to the two profiles measured at the beginning and the end of the field season 1992. Figure 2 shows that the temperature difference in the depth range of 50-

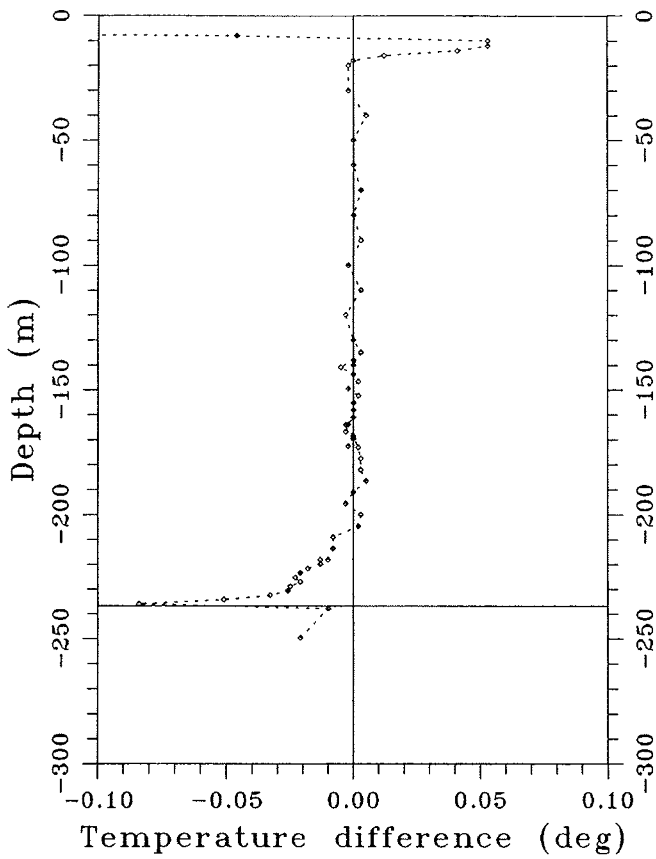

Fig. 2: Difference between the temperature profiles from 20-02-1992 and 25-01-1992 at the ice edge of FRIS.

Abb. 2: Differenz der Temperatur-Tiefenprofile vom 20.02.1992 and 25.01.1992 im Kantenbereich des FRIS.

200 m is zero, with respect to the relative resolution of 0.003 K of the temperature measurement. The basal temperature during these 26 days rises by 0.084 K, which is a significant quantity for the calculation of bottom melting in the summer period. Using the same interpolation method for the basal temperature gradient, a melting rate of m = -2.53 ±2.12 m/a can be derived.

This result might be a hint for a seasonal change of the melting rate superposed on the mean melting rate, which can be derived from the long-term measurement and which is caused by the in- or outflow of sea water above its *in situ* freezing point. The two measurements 1992, however, were taken during the summer months when the coastal polynya of the Weddell Sea was open. During this period an optimal interaction between atmosphere and ocean is possible causing an additional heat input into the ocean water. Regional circulations and ocean tides can therefore provide the input of relatively warm sea water with a potential for melting underneath the ice shelf (GAMMELSRØD & SLOTSVIK 1981). In addition ice pumping processes, like those described by LEWIS & PERKIN (1986), represent an effective mechanism for melting near the ice edge, since water at the surface freezing point penetrates to greater depth and pressures, where the interaction with colder ice at the *in situ* freezing point causes melting with high amplitudes.

To demonstrate the influence of regional circulation underneath the ice shelf a continuous record (sampling rate of 2 min) of the lowest four PT100-sensors with a spacing of about 2 m is shown in Figure 3. The two sensors no. 248 and no. 250 reach into the sea water, while sensors no. 244 and no. 246 were placed near the bottom in the ice shelf. The registration of sea-water temperatures show distinct diurnal and semidiurnal tides with amplitudes between 0.025 K and 0.14 K. The variation in amplitude refers to a strong modulation of different partial tides, which were calculated from the amplitude spectra of the time series (Fig. 4). The constituents of this analysis are the diurnal (O1, K1) and the semidiurnal (M2, S2) tides. The 14-days tide (M_f) could not be seperated clearly, because the registration time of 26 days was too short.

In the plot of temperatures (Fig. 3) a strong correlation between the amplitudes of the ocean tides and the heat flux into the ice can be recognized, indicated by the changing mean temperature gradient of element no. 246. From simple modelling of heat conduction in a medium subjected to a harmonic change of temperatures (PATERSON 1981) it can be shown that the high-frequency part of the stimulating temperature wave fades faster than the low frequency part. However, the large amplitudes of the diurnal and semidurnal tides are responsible for the input of warm sea water under the ice shelf and thus for bottom melting. The rate of change in temperature of sensor no. 246, which is positioned next to the ice-shelf bottom, correlates with the amplitude of the temperature variation of the sea water (sensor no. 248). Deeper in the ice (sensor no. 244) this effect has faded away to a constant heat flux causing a linear temperature gradient during the registration period.

The mean temperature of sensor no. 248 placed in the ocean next to the ice-shelf bottom is -2.033° C, the mean temperature of sensor no. 250, 2 m below, is -1.887° C (Fig. 3, dotted lines). Since the amplitudes of both registrations are nearly the same, their absolute values differ constantly by about 0.146 K. This cooling of the sea water underneath the ice shelf is obviously caused by the input of meltwater and its mixture with water circulating under the ice shelf from or to the open sea. In addition, there seems to be a minimum of the sea-water temperature in both depths, respectively, at fixed temperatures which depend on the salinity of the sea water in these layers. In contrast to that the maximum temperatures vary with different tides and depend on the absolute heat input of the inflowing sea water. Hence, these measurements can contribute to the understanding of the complex process of ice shelf/ocean interaction.

TDR MEASUREMENTS

In addition to the temperature measurements, sensor lines for time-domain reflectometry (TDR) measurements were installed. This technique is based on travel-time measurements of a short pulse transmitted on parallel sensor lines and reflected at dielectric discontinuities of its surrounding medium. The design of the system and the results of the initial recordings at the end of the field season 1989/90 are described by GROSFELD & BLINDOW (1993). In this paper the results from the re-measurement and a derived bottom-melting rate are discussed. Figure 5 shows an

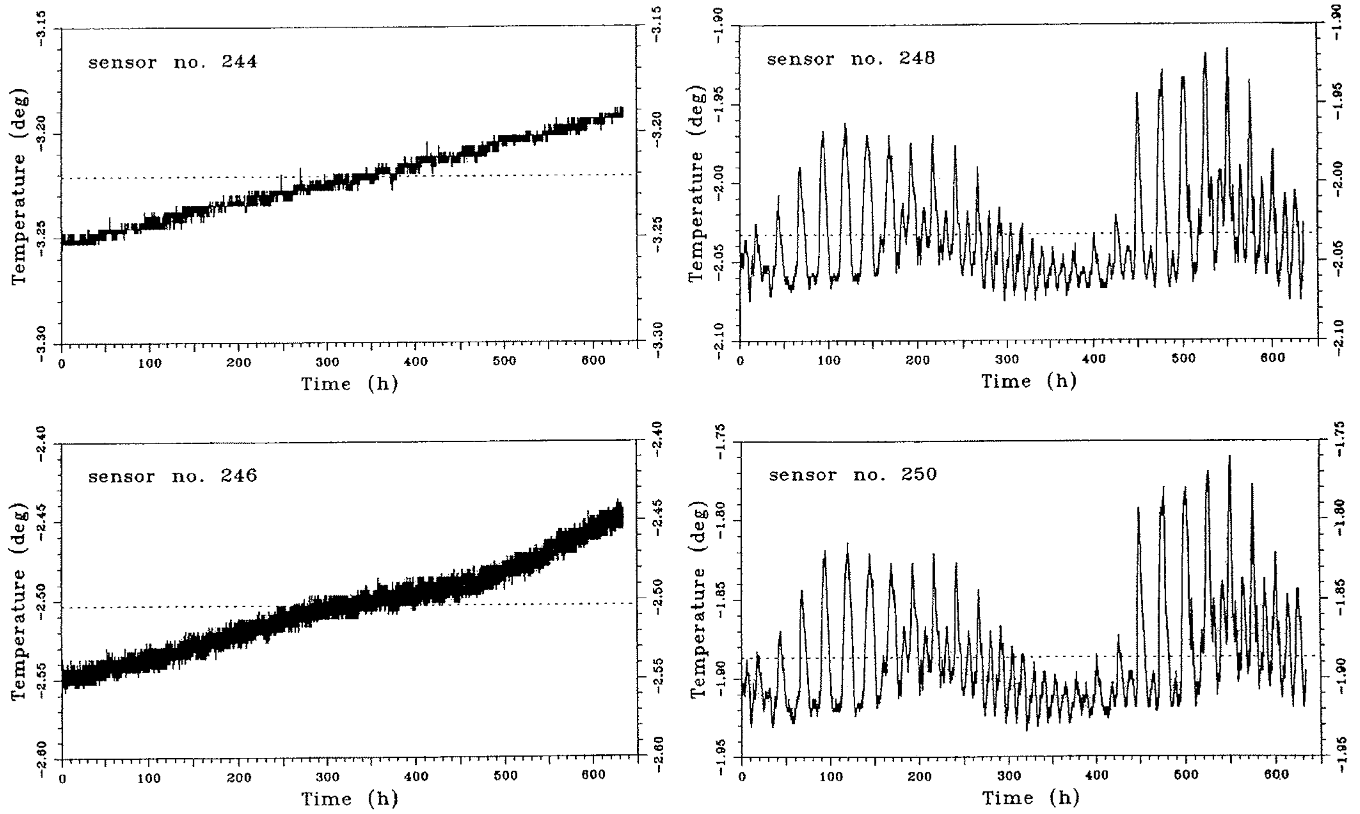

Fig. 3: Continuous temperature record of the lowest four PT100-sensors with a spacing of about 2 m. Sensors no. 248 and no. 250 are positioned in the sea water under the ice shelf, while sensors no. 244 and no. 246 are positioned in the ice shelf itself.

Abb. 3: Kontinuierliche Temperaturregistrierung der unteren vier PT100-Meßsensoren in einem Tiefeninkrement von etwa 2 m. Die Sensoren Nr. 248 und Nr. 250 befinden sich direkt unterhalb des Schelfeises im Meerwasser, während die Sensoren Nr. 244 und Nr. 246 noch im Schelfeis plaziert sind.

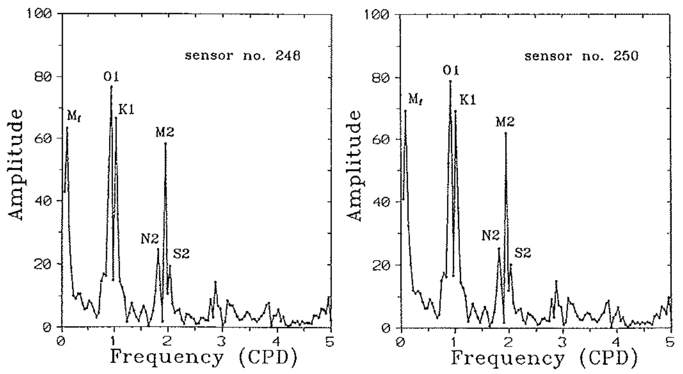

Fig. 4: Amplitude spectra of the temperature registrations of sensor no. 248 und no. 250 in the sea water.

Abb. 4: Amplitudenspektren der Temperaturregistrierungen der im Meerwasser befindlichen Meßsensoren Nr. 248 und Nr. 250.

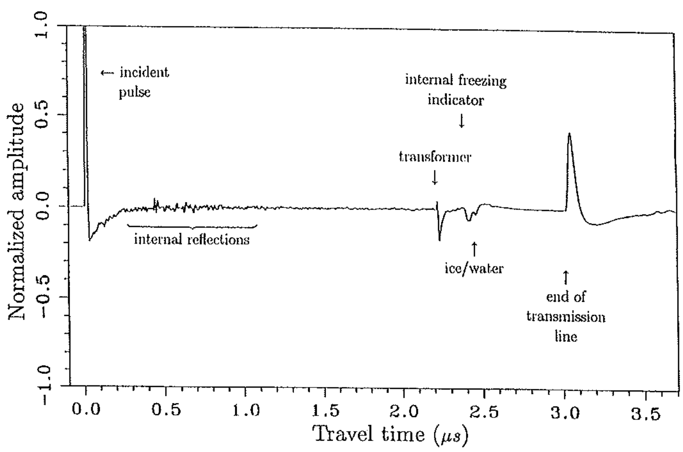

Fig. 5: Example of a TDR-measurement of an installed sensor line for the direct determination of the basal melting rate. The sensor line is composed of 220 m of coaxial line and 60m of 240 Ω stripline; registration 30 dB amplificated.

Abb. 5: Beispiel einer TDR-Registrierung an einer im FRIS installierten Sensorleitung zur direkten Bestimmung der basalen Schmelzrate. Die Sensorleitung besteht aus 220 m Koaxialkabel und 60 m 240 Ω-Zweidrahtleitung; Registrierung 30 dB verstärkt.

example of a recorded waveform of 1992. Since the first 220 m of the cable are shielded, the time interval up to 2.2 μs after the incident pulse is not influenced by its surroundings. The first detectable reflection signal is caused by the RF-transformer which connects the coaxial cable and sensor line (240 Ω stripline). The travel-time interval up to the end of the stripline (t = 3.008 μs) is marked with two distinct reflections, one of the ice/sea-water boundary at 2.433 μs and another one of an internal freezing layer at 2.374 μs. The explanation for the latter was a freezing horizon caused by sea water penetrating into the borehole after the piercing of the ice shelf. From the 1990 data we expected that this signal would be reduced or would vanish in favour of the signal from the ice-shelf bottom. Instead, the largest signal in amplitude of the year 1990 splits into a double-peak signal and influences the onset of the bottom-reflection. For this reason the reflection signal from the ice-shelf bottom can not be determined with the expected quality in onset picking (one sample point of the reflection signal from the ice/sea-water boundary) as expected from the 1990 data (GROSFELD & BLINDOW 1993).

In spite of that, the re-measurement of the installed TDR cable gives a value for the basal melting rate with only minor accuracy using the following concept: Assuming comparable freezing conditions in the lower part of the borehole in both years of measurements, the difference of travel times Δt between the reference signal (transformer) and the end of the sensor line can be evaluated. It depends on the proportion of the propagation velocities along the stripline in the sea water and the ice shelf. A schematic diagram of this concept is shown in Figure 6. The symbols v_i and v_w denote the propagation velocities of the pulse in ice and water, H_i and H_w the thickness of the ice column from the transformer to the ice-shelf bottom and of the water column between the ice-shelf bottom and the end of the stripline. ΔH is the thickness of the layer melted away in the time interval between the two measurements. If the travel-time difference between the transformer and the end of the stripline can be determined from both measurements in 1990 and 1992, the bottom-melting rate can be calculated from the reciprocal propagation velocity in ice and sea water.

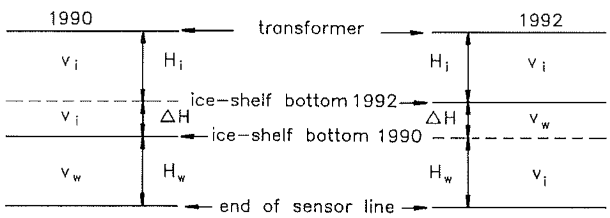

$$t_1 = 2 * \left(\frac{H_i}{v_i} + \frac{\Delta H}{v_i} + \frac{H_w}{v_w} \right) \qquad t_2 = 2 * \left(\frac{H_i}{v_i} + \frac{\Delta H}{v_w} + \frac{H_w}{v_w} \right)$$

$$\Delta t = t_2 - t_1 = 2 \Delta H * \left(\frac{1}{v_w} - \frac{1}{v_i} \right)$$

Fig. 6: Schematic diagram for the determination of the bottom-melting rate from a two-years re-measurement with TDR-devices.

Abb. 6: Schemazeichnung des Auswertekonzeptes zur Bestimmung der basalen Schmelzrate aus TDR-Messungen im Abstand von zwei Jahren.

From a travel-time difference of 11±2 ns between 1990 and 1992 and propagation velocities v_i = 194 ±2 m/µs and v_w = 141±2 m/µs, the bottom-melting rate over a period of 737 days is m = -1.41±0.45 m/a. This value agrees quite well with the long-term determination from temperature measurements and represents an independent examination of the little known mass-balance parameter.

MASS-BALANCE STUDY

A third method for the determination of the basal melting rate was used in the same area during the 1989/90 field season. As a joint project of geophysicists, geodesists and field glaciologists, a specialy designed strain network was investigated to derive the necessary quantities for the calculation of bottom melting from the mass-conservation equation. The design of this experiment and its results is described in detail separately (DETERMANN et al. 1990). The geometry and size of the experiment was planned on such a scale that a result with high accuracy could be obtained within a single field season. Although the field studies were carried out within a short-time period, the integration over a grid size of 10•10 km gave an overall melting rate of m = -1.50 ±0.15 m/a, which represents a mean value over a larger time scale under consideration of steady-state conditions.

CONCLUSIONS

Summing up these independent determinations of the bottom-melting rate a consistent result of this little known mass-balance parameter is obtained for the ice-edge region of the western FRIS:

- A direct observation of bottom melting is possible from temperature measurements in boreholes. Installed temperature chains yield
  (a) a rough measurement by the amount of temperature sensors melted out of the ice-shelf bottom (-1.0 m/a ≥ m > -2.0 m/a);
  (b) a more accurate value from the bottom-temperature gradient (m = -1.28 ±0.24 m/a).

In addition to (b), small temperature variations indicate a seasonal dependence of the bottom-melting rate (m = -2.53 ±2.12 m/a) during a period of 26 days in the summer field season. The temperature measurements in the sea water underneath the ice shelf show strong tidal effects as important factors for ice/ocean interactions.

- Time-domain reflectometry measurements are an independent tool for a direct determination of bottom melting. From travel-time measurements the melting of the ice-shelf bottom can be observed in relation to a reference level. With this technique a bottom-melting rate of m = -1.41 ±0.45 m/a was derived. Indeed, the expected accuracy in resolution could not be achieved, but a melting rate within an acceptable error limit can be evaluated. However, a special registration technique can yield data with higher accuracy.

- From a surface-based mass-balance study an indirect estimation of the bottom-melting rate is attained. From this experiment a melting rate of m = -1.50 ±0.15 m/a was determined within a single field season (DETERMANN et al. 1990). Strain determinations over a large area and ice thickness measurements with high accuracy compensate for the small time interval.

Classifying the different experiments and their results, the indirect surface measurement can yield a sufficient accurate value for the bottom-melting rate compared with borehole measurements. TDR-measurements in boreholes do not give a more exact quantity, they only confirm the indirect determination with direct observations and provide evidence of steady state conditions. In addition it makes possible an examination of the re-freezing process of the borehole itself.

The consuming technique of hot-water drilling is worthwhile for the deployment of thermistor chains. Temperature measurements in boreholes yield data of much more detail and speciality in relation to bottom-melting and its processes. With regard to ice/ocean interactions as a response to global changes, long-term temperature studies in boreholes in combination with oceanographic measurements under ice shelves are a useful tool for the examination of the equilibrium and stability of the Antarctic ice shelves.

ACKNOWLEDGEMENTS

Special thanks are due to Dr. Josef Kipfstuhl (Alfred Wegener Institute for Polar and Marine Research, AWI) who did the re-measurements of the installed chains and the installation of our data-logging equipment in 1992. Logistic support by the AWI is gratefully acknowledged. This work was funded by the Deutsche Forschungsgemeinschaft (DFG, grants TH168/20-2 and BL307/1-1) and the Land Nordrhein-Westfalen.

References

Behrendt, J.C. (1970): The structure of the Filchner Ice Shelf and its relation to bottom melting.- IASH 86: 488-496.

Determann, J., Grosfeld, K. & Ritter, B. (1990): Melting rates at the bottom of Filchner-Ronne Ice Shelf, Antarctica, from short-term mass-balance studies.- Polarforschung, 60: 25-32.

Drewry, D.J., Jordan, S.R. & Jankowski, E. (1982): Measured properties of the Antarctic Ice Sheet: surface configuration, ice thickness, volume and bedrock characteristics.- Annals Glaciology 3: 83-91.

Foldvik, A. & Kvinge, T. (1974): Conditional instability of sea water at the freezing point.- Deep Sea Res. 21: 169-174.

Foldvik, A., Gammelsrød, T & Tørresen, T. (1985): Circulation and water masses on the southern Weddell Sea Shelf.- In: S.S. Jacobs (ed.), Oceanology of the Antarctic Continental Shelf, Antarctic Research Series 43, 5-20, AGU Washington DC.

Gammelsrød, T. & Slotsvik, N. (1981): Hydrographic and current measurements in the southern Weddell Sea 1979/80.- Polarforschung 51: 101-111.

Grosfeld, K. (1993): Untersuchungen zu Temperaturregime und Massenhaushalt des Filchner-Ronne-Schelfeises, Antarktis, unter besonderer Berücksichtigung von Anfrier- und Abschmelzprozessen.- Berichte Polarforsch. 130, pp. 148.

Grosfeld, K. & Blindow, N. (1993): Determination of ice shelf bottom melting by time domain reflectometry.- Journal Glaciology 39(132): 353-356.

Jenkins, A. & Doake, C.S.M. (1991): Ice-ocean interaction on Filchner-Ronne Ice Shelf, Antarctica.- J. Geophys. Res. 96(C1): 791-813.

Kohnen, H. (1982): Glaciological investigation in the frontal zone of the Filchner and Ronne Ice Shelf.- Annals Glaciology 3: 160-165.

Paterson, W.S.B. (1981): The Physics of Glaciers.- Pergamon Press, 2nd Edition, Oxford, New York, Toronto, Sydney, Paris, Frankfurt.

Lewis, E.L. & Perkin, R.G. (1986): Ice pumps and their rates.- J. Geophys. Res. 91(C10): 11756-11762.

Thyssen F. (1988): Special aspects of the central part of Filchner-Ronne Ice Shelf, Antarctica.- Annals Glaciology 11: 173-179.